

1  
2  
3 1 Title: **Cell adhesive peptides functionalized on CoCr alloy stimulate**  
4  
5 2 **endothelialization and prevent thrombogenesis and restenosis**  
6  
7 3

8  
9 4 Authors: Maria Isabel Castellanos<sup>1,2</sup>, Jordi Guillem-Marti<sup>1,2</sup>, Carlos Mas-Moruno<sup>1,2</sup>,  
10  
11 5 Maribel Díaz-Ricart<sup>3</sup>, Ginés Escolar<sup>3</sup>, Maria Pau Ginebra<sup>1,2,4</sup>, Francisco Javier  
12  
13 6 Gil<sup>5</sup>, Marta Pegueroles<sup>1,2\*</sup>, Jose María Manero<sup>1,2\*</sup>  
14  
15 7

16  
17 8 Affiliations: <sup>1</sup> Biomaterials, Biomechanics and Tissue Engineering Group, Department of  
18  
19 9 Materials Science and Metallurgical Engineering, ETSEIB, Technical  
20  
21 10 University of Catalonia (UPC), 08028 Barcelona, Spain  
22

23 11 <sup>2</sup> Centre for Research in NanoEngineering (CRNE), UPC, 08028 Barcelona,  
24  
25 12 Spain  
26

27 13 <sup>3</sup> Hemotherapy-Hemostasis Department, Centre de Diagnòstic Biomèdic,  
28  
29 14 Institut d'Investigacions Biomèdiques August Pi i Sunyer (IDIBAPS), Hospital  
30  
31 15 Clinic, Universitat de Barcelona, 08036 Barcelona, Spain  
32

33 16 <sup>4</sup> Institute for Bioengineering of Catalonia (IBEC), 08028 Barcelona, Spain  
34

35 17 <sup>5</sup> Universitat Internacional de Catalunya (UIC), 08017 Barcelona, Spain  
36  
37 18

38  
39 19 Corr. Author: José Maria Manero, PhD

40  
41 20 [jose.maria.manero@upc.edu](mailto:jose.maria.manero@upc.edu)

42  
43 21 Department of Materials Science and Metallurgical Engineering

44  
45 22 Av. Diagonal, 647

46  
47 23 Barcelona, 08028

48  
49 24 Spain.  
50

51  
52 25  
53  
54 26 Marta Pegueroles, PhD

55  
56 27 [marta.pegueroles@upc.edu](mailto:marta.pegueroles@upc.edu)

57  
58 28 Department of Materials Science and Metallurgical Engineering  
59  
60

1  
2  
3 1 Av. Diagonal, 647  
4  
5 2 Barcelona, 08028  
6  
7 3 Spain.  
8  
9 4 Maria Isabel Castellanos: [maria.isabel.castellanos@upc.edu](mailto:maria.isabel.castellanos@upc.edu)  
10  
11 5 Jordi Guillem-Marti: [jordi.guillem.marti@upc.edu](mailto:jordi.guillem.marti@upc.edu)  
12  
13 6 Carlos Mas-Moruno: [carles.mas.moruno@upc.edu](mailto:carles.mas.moruno@upc.edu)  
14  
15 7 Maribel Díaz-Ricart: [mdiaz@clinic.ub.es](mailto:mdiaz@clinic.ub.es)  
16  
17 8 Ginés Escolar: [gescolar@clinic.ub.es](mailto:gescolar@clinic.ub.es)  
18  
19 9 Maria Pau Ginebra: [maria.pau.ginebra@upc.edu](mailto:maria.pau.ginebra@upc.edu)  
20  
21 10 Francisco Javier Gil: [xavier.gil@uic.cat](mailto:xavier.gil@uic.cat)  
22  
23 11 Marta Pegueroles: [marta.pegueroles@upc.edu](mailto:marta.pegueroles@upc.edu)  
24  
25 12 Jose María Manero: [jose.maria.manero@upc.edu](mailto:jose.maria.manero@upc.edu)  
26  
27  
28  
29  
30  
31  
32  
33  
34  
35  
36  
37  
38  
39  
40  
41  
42  
43  
44  
45  
46  
47  
48  
49  
50  
51  
52  
53  
54  
55  
56  
57  
58  
59  
60

**Abstract**

Immobilization of bioactive peptide sequences on CoCr surfaces is an effective route to improve endothelialization, which is of great interest for cardiovascular stents. In this work, we explored the effect of physical and covalent immobilization of RGDS, YIGSR and their equimolar combination peptides on endothelial cells (EC) and smooth muscle cell (SMC) adhesion and on thrombogenicity. We extensively investigated using RT-qPCR, the expression by ECs cultured on functionalised CoCr surfaces of different genes. Genes relevant for adhesion (ICAM-1 and VCAM-1), vascularization (VEGFA, VEGFR-1 and VEGFR-2) and anti-thrombogenicity (tPA and eNOS) were over-expressed in the ECs grown to covalently functionalized CoCr surfaces compared physisorbed and control surfaces. Pro-thrombogenic genes expression (PAI-1 and vWF) decreased over time. Cell co-cultures of ECs/SMCs found that functionalization increased the amount of adhered ECs onto modified surfaces compared to plain CoCr, independently of the used peptide and the strategy of immobilization. SMCs adhered less compared to ECs in all surfaces. All studied peptides showed a lower platelet cell adhesion compared to TCPS. Covalent functionalization of CoCr surfaces with an equimolar combination of RGDS and YIGSR represented prevailing strategy to enhance the early stages of ECs adhesion and proliferation, while preventing SMCs and platelet adhesion.

**Key Words**

Functionalization; CoCr alloy; gene expression; platelet adhesion; cell co-culture

1  
2  
3 **Short title: CELL ADHESIVE PEPTIDES FUNCTIONALIZED ON CoCr ALLOY**  
4  
5  
6

7 **INTRODUCTION**  
8

9 Atherosclerosis, the hardening of arteries due to build-up of lipoproteins, is one of the leading  
10 causes of death worldwide.<sup>1-3</sup> One of the most common treatments for vessel occlusion due to  
11 atherosclerotic lesion formation is stent implantation where the stent is expanded in the  
12 narrowed artery recovering blood flow. While stenting has become a widely used procedure, it  
13 is not without complications.  
14  
15

16 In-stent restenosis<sup>4</sup> and late stent thrombosis<sup>5</sup> are the main drawbacks of actual bare metal stents  
17 (BMS)<sup>6</sup> and drug-eluting stents (DES),<sup>4</sup> respectively. In-stent restenosis is due to the body's  
18 own wound healing response to the mechanical injury associated with stent implantation<sup>7</sup> where  
19 increased proliferation of smooth muscle cells (SMCs) leads to renarrowing of the arteries.<sup>8</sup>  
20 Late stent thrombosis might be related to a delay in re-endothelialization following stenting,  
21 which has been shown in pathology studies.<sup>9</sup> A stent surface rapid endothelialization minimizes  
22 the failures associated with blood clotting and platelet activation<sup>10</sup> and is expected to reduce in-  
23 stent restenosis. The rate and quality of endothelialization of a stent depend on interactions  
24 between endothelial cells (ECs) with the biomaterial surface.  
25  
26

27 Material surface properties can be modified by physicochemical modification and/or  
28 biofunctionalization to promote EC adhesion and inhibit thrombosis by influencing protein  
29 adsorption and subsequent cell behavior.<sup>11,12</sup> But, in the recent years, there is a growing interest  
30 in the immobilization of bioactive molecules on the surface of biomaterial implants through  
31 covalent bonding.<sup>13,14</sup> Covalent functionalization is based on the formation of a covalent linkage  
32 between functional entities and the material surface. The advantages of the process includes  
33 control of molecular orientation, minimization of non-specific interactions, and greater stability  
34 of the functional surface by preventing dissolution, desorption, and degradation of molecules.<sup>15</sup>  
35  
36 However, the optimal sequences and their combinations remain to be elucidated.  
37  
38  
39  
40  
41  
42  
43  
44  
45  
46  
47  
48  
49  
50  
51  
52  
53  
54  
55  
56  
57  
58  
59  
60

1  
2  
3 1 The inner arterial wall of the entire vascular system consist of a continuous single layer of ECs  
4  
5 2 which separates blood from the vessel wall.<sup>16</sup> The endothelium regulates the transfer of  
6  
7 3 molecules, such as lipoproteins, between the blood and vessel wall and acts as a semipermeable  
8  
9 4 barrier.<sup>17,18</sup> In addition to serving as a physical barrier, ECs also control many important  
10  
11 5 functions in vascular homeostasis including vascular tone, inflammation, and lipid and tissue-  
12  
13 6 fluid homeostasis, and has antithrombotic properties.<sup>18</sup> The antithrombotic and anticoagulant  
14  
15 7 balance is maintained through processes involving nitric oxide production, prostacyclin, tissue  
16  
17 8 plasminogen activator, thrombomodulin, heparin-like molecules, tissue-factor pathway inhibitor  
18  
19 9 and many other molecules.<sup>9</sup> Designed biomaterial should stimulate ECs adhesion and migration  
20  
21 10 and prevent SMCs adhesion and proliferation in order to obtain a functional artery.

22  
23 11 Based on previous results of functionalized CoCr alloy surfaces with RGDS, REDV and YIGSR  
24  
25 12 peptides, we find that peptides immobilization, specially the combination of RGDS and YIGSR,  
26  
27 13 represent a good strategy to enhance initial EC adhesion and migration.<sup>19</sup> The bioactivity of  
28  
29 14 these peptides has been thoroughly demonstrated by scrambling their sequences.<sup>20-22</sup> Now we  
30  
31 15 would like to go a step further by studying the effect of functionalized CoCr surfaces on gene  
32  
33 16 expression of EC. Specifically, expression profiles of nine gene markers, related with four  
34  
35 17 different functions of EC: adhesion (ICAM-1 and VCAM-1), vascularization (VEGFA,  
36  
37 18 **VEGFR-1** and VEGFR-2), pro thrombogenic (PAI-1 and vWF) and anti-thrombogenic genes  
38  
39 19 (eNOS and tPA) were analyzed by real time quantitative polymerase chain reaction (RT-qPCR).  
40  
41 20 Also, we have evaluated thrombogenicity of the peptides by quantifying platelet adhesion and  
42  
43 21 aggregation under defined shear stress conditions.<sup>23</sup>

44  
45 22 Moreover, a co-culture system has been performed by plating EC and SMC together in tissue  
46  
47 23 culture to evaluate the rapid competitive adhesion, proliferation and migration of ECs and  
48  
49 24 SMCs to identify the aspects of the modified CoCr surfaces, which favor re-endothelialization  
50  
51 25 while alongside inhibiting the SMCs proliferation and platelet adhesion.

52  
53  
54 26

## 55 56 27 **MATERIAL AND METHODS**

### 57 58 28 **Metallic surface**

1  
2  
3 1 Comercial CoCr alloy discs (8.5 mm in diameter, 2-3 mm thick) were obtained from CoCr alloy  
4 (ASTM F90) bars (Technalloy S.A., Barcelona, Spain). Samples were polished to achieve  
5 2  
6 mirror-like, smooth surfaces by grinding with abrasive SiC papers (Neuertek S.A., Eibar and  
7 3  
8 Beortek S.A., Asua-Erandio, Spain) of decreasing grit size (P600, P800 and P1200), followed  
9 4  
10 by polishing with suspension of alumina particles (1  $\mu\text{m}$  and 0,05  $\mu\text{m}$ ). Prior to  
11 5  
12 biofuncionalization, all samples were ultrasonically rinsed with ethanol, distilled water and  
13 6  
14 acetone and stored dried.  
15 7  
16

### 17 8

### 19 **Solid-phase peptide synthesis**

20 9  
21 10 The linear peptides MPA-(Ahx)<sup>3</sup>-Arg-Gly-Asp-Ser-OH (RGDS) and MPA-(Ahx)<sup>3</sup>-Tyr-Ile-  
22 11  
23 Gly-Ser-Arg-OH (YIGSR) (Ahx: aminohexanoic acid; MPA: 3-mercaptopropionic acid) were  
24 12  
25 manually synthesized by solid-phase following the Fmoc/tBu strategy and using CTC resin (200  
26 13  
27 mg, 1.0 mmol/g) as previously reported.<sup>24</sup> The purified peptides were characterized by  
28 14  
29 analytical HPLC analysis and MALDI-TOF. All chemicals required for the synthesis, including  
30 15  
31 resins, Fmoc-L-amino acids and coupling reagents, were obtained from Iris Biotech GmbH  
32 16  
33 (Marktredwitz, Germany) and Sigma-Aldrich (St Louis, MO, USA).  
34 17  
35

### 36 18 **Cell culture**

37 19  
38 20 Human umbilical vein endothelial cells (HUVECs) were cultured in EC basal medium (EBM®)  
39 21  
40 supplemented with EGM-2 BulletKit and 5% (v/v) fetal bovine serum (FBS). Human vascular  
41 22  
42 coronary artery smooth muscle cells (CASMCs) were grown in SMC basal medium (SmBm®)  
43 23  
44 supplemented with SmGM-2 BulletKit and 5% (v/v) FBS. All cells, mediums and supplements  
45 24  
46 were purchased from Lonza (Basel, Switzerland). Cells were maintained at 37°C, in a humified  
47 25  
48 atmosphere containing 5% (v/v) CO<sub>2</sub> and culture medium was renewed every 2 days. Cell  
49 26  
50 culture was performed in Nunc cell flasks (Thermo Scientific, Denmark) pre-coated with  
51 27  
52 1  $\mu\text{g}/\text{ml}$  of human plasma fibronectin (Sigma-Aldrich) in PBS. HUVECs at passages 4 to 8<sup>3,13</sup>  
53 28  
54 and CASMCs at passages 4 to 6<sup>25,26</sup> were used in all the experiments.  
55 29  
56  
57  
58  
59  
60

### 1 **Biofunctionalization of CoCr surfaces**

2 Prior to silanization, CoCr samples were activated by alkaline etching with 5M NaOH for 2  
3 hours and after, samples were thoroughly cleaned by immersion in distilled water for 30 min  
4 twice. After activation the samples were introduced in a N<sub>2</sub>-saturated glass vessel and immersed  
5 for 1 h at 90°C in a solution containing 0,5 M 3-chloropropyltriethoxysilane (CPTES) and 0,05  
6 M N,N-diisopropylethylamine (DIEA) in anhydrous toluene (Sigma-Aldrich) under nitrogen  
7 atmosphere. Next, samples were ultrasonicated successively in cyclohexane, isopropanol,  
8 distilled water and acetone, and finally dried with N<sub>2</sub> gas.

9 Biomolecules were immobilized on the CoCr surfaces by two different methods: (1) physical  
10 adsorption on plain CrCo samples (samples were coded as CT+peptide); and (2) covalent  
11 immobilization through silanization process of the CoCr activated surfaces with CPTES  
12 (samples coded as NA-CP+peptide).

13 The RGDS, YIGSR peptides and their combination (1:1) were dissolved in a solution of  
14 phosphate buffered saline (PBS) adjusted with Na<sub>2</sub>CO<sub>3</sub> to obtain a pH of 13.0 at a concentration  
15 of 100 µM. 100 µl of peptide solutions were deposited on the CPTES-grafted surfaces overnight  
16 at room temperature (RT). To adsorb physically the peptide on non-silanized samples, the same  
17 conditions were used but using PBS at pH 7.4 instead. Control samples were only treated with  
18 buffer. After peptide incubation, samples were gently washed three times with distilled water  
19 and dried with nitrogen.

20 The biofunctionalized samples, and their controls, are codified as follows:

21 **CT:** Non-treated smooth CoCr surface.

22 **CT-RGDS:** CoCr surface coated with 100 µM of RGDS peptide.

23 **CT-YIGSR:** CoCr surface coated with 100 µM of YIGSR peptide.

24 **CT-RGDS+YIGSR:** CoCr surface coated with 100 µM of RGDS+YIGSR combined peptides.

25 **NA-CP-RGDS:** CoCr activated with NaOH, silanized with CPTES and coated with 100 µM of  
26 RGDS peptide.

27 **NA-CP-YIGSR:** CoCr activated with NaOH, silanized with CPTES and coated with 100 µM of  
28 YIGSR peptide.

1 **NA-CP-RGDS+YIGSR:** CoCr activated with NaOH, silanized with CPTES and coated with  
2 100  $\mu$ M of RGDS+YIGSR combined peptides.

3 Prior to cell adhesion assays, functionalized samples were blocked for 1 h at 37 ° C with 5%  
4 (w/v) bovine serum albumin (BSA) in PBS in order to reduce non-specific interactions of the  
5 cells with the surface.<sup>24,27-29</sup>

### 7 **Quantitative real-time polymerase chain reaction**

8 Expression of adhesion (ICAM-1, VCAM-1), vascularization (VEGFA, VEGFR-1, VEGFR-2),  
9 pro-thrombogenic (vWF, PAI-1) and anti-thrombogenic (tPA, eNOS) genes (Table 1) in  
10 HUVECs on modified CoCr surfaces was determined through RT-qPCR assay after 24 h, 48 h  
11 and 72 h as previously described.<sup>30</sup>

12 At each culture time, total RNA was extracted using RNeasy® Mini Kit (Qiagen, Hilden,  
13 Germany) and quantified using a NanoDrop ND-1000 spectrophotometer (NanoDrop  
14 Technologies, Montchanin, DE, USA). One hundred nanograms were retrotranscribed to cDNA  
15 products which were further diluted and used as RT-qPCR templates (Quantitect Reverse  
16 Transcription Kit, Qiagen). The resulting cDNA is then amplified using the QuantiTect SYBR  
17 Green RT-qPCR Kit (Qiagen) in an ABIPrism 7700 machine (Applied Biosystems, Foster City,  
18 CA, USA). Specificity of each RT-qPCR reaction was determined by melting curve analysis and  
19 by resolving the RT-qPCR products on 2% agarose gels. The expression of all studied genes  
20 was normalized by the expression levels of  $\beta$ -actin. Moreover, fold changes were related to CT  
21 at 24 h of culture.

### 23 **Platelet adhesion**

24 Platelet activation and adhesion on the peptides were evaluated by exposing human blood to  
25 physiological arterial shear stress. Peptides were physisorbed into a commercially available  
26 cone and plate-shearing device (Diamed Impact-R; Biorad Diamed GmbH, Cressier,  
27 Switzerland). The Impact-R [Cone and plate(let) analyzer] is designed to evaluate platelet  
28 function under flow conditions.<sup>31</sup> Samples of citrate phosphate dextrose (CPD) anti-coagulated



1 whole blood (130  $\mu$ l) were placed on polystyrene wells and subjected to flow at 1800  $s^{-1}$  for 2  
2 min using a specially designed conical disk. Wells were then thoroughly washed with PBS,  
3 stained with May-Gruenwald stain and analyzed by the Impact-R analyzer system connected to  
4 a microscope. Platelet adhesion was determined by measuring the percentage of the well surface  
5 covered with platelets and the average size of the aggregates.

### 7 **Immunofluorescence analysis of HUVECs and CASMCs co-culture**

8 The HUVECs and CASMCs were separately grown until confluence. Then, a direct cell contact  
9 co-culture was performed by seeding onto the modified CoCr surfaces  $10^4$  cells/well HUVECs  
10 and  $10^4$  cells/well CASMCs in mixed EBM® and SmBm® (1:1) free-serum medium. After 24  
11 h, the serum-free medium was changed by complete EBM® and SmBm® (1:1) medium until  
12 analysis. To discriminate cells by immunofluorescence, two specific cell-markers were used:  
13 PECAM-1 platelet endothelial cell adhesion molecule (CD31, Sigma Aldrich) for staining  
14 HUVECs and  $\alpha$ -SMA  $\alpha$ -smooth muscle actin (A5228, Sigma Aldrich) for staining CASMCs.  
15 Cells were fixed in a mixture of ethanol-acetone (50:50, v/v)<sup>32</sup> for 30 min, permeabilized with  
16 0.05% (v/v) Triton X-100 in PBS for 20 min and blocked with 1% BSA (w/v) in PBS for 30  
17 min. HUVECs and SMCs were stained by incubating first with the primary antibodies mouse  
18 anti-PECAM-1 (1:100, in blocking solution) and rabbit anti- $\alpha$ -SMA (1:100 in blocking  
19 solution) for 1 h. Finally cells were stained by incubation with the secondary antibodies Alexa  
20 Fluor 488 chicken anti-rabbit (Sigma Aldrich) and Alexa Fluor 568 goat anti-mouse (Sigma  
21 Aldrich), during 1 h in the dark. Nuclei were counterstained with DAPI (1:1000, in PBS) for 10  
22 min in the dark. Between all steps, samples were rinsed twice with PBS for 5 min. CoCr disks  
23 were mounted and examined under a fluorescent inverted microscope (AF6500 widefield, Leica  
24 Microsystems, Germany) where images through stitching method were taken. Cell number and  
25 morphology were studied by ImageJ-FIJI software (NIH, USA).

### 27 **Statistical analysis**

1 All the experiments were triplicated for each condition and repeated at least in two independent  
2 experiments. Statistical comparison of values was based on ANOVA using Tukey's test for pair-  
3 wise comparison with  $p < 0.05$ . Differences were also analyzed by non-parametric Kruskal-  
4 Wallis test. Values of all graphs are reported as mean  $\pm$  standard deviation. Statistical analysis  
5 was performed using Minitab software (Minitab Inc., USA).

## 7 **RESULTS**

### 8 **Cell adhesion gene expression**

9 The expression of genes related to cell adhesion (ICAM-1 and VCAM-1) was analysed at 24, 48  
10 and 72 h on the different functionalized CoCr surfaces by real time – qPCR (Fig. 1). ICAM-1  
11 gene expression was enhanced in HUVEC cultured on silanized CoCr surfaces, Na-CP series,  
12 after 48 h and even more upregulated after 72 h. Nonetheless, physisorbed series only presented  
13 a slightly increase of ICAM-1 expression after 48 and 72 h compared to plain CoCr, CT. From  
14 all tested surfaces NA-CP-RGDS+YIGSR was the functionalized CoCr substrate with a higher  
15 expression of ICAM-1 after 48 and 72 h. VCAM-1 gene expression showed an upregulation of  
16 its expression after 48 h specially for silanized series, whereas it was significantly decreased after  
17 72 h for all tested surfaces [Fig. 1(b)].

### 19 **Vascularization gene expression**

20 It was investigated the effect of immobilization of adhesive molecules onto CoCr, by  
21 physisorption or covalent binding, on the activation of HUVECs gene expression levels for  
22 vascularization through the analysis of VEGFA, VEGFR-1 and VEGFR-2 gene expression (Fig.  
23 2). The gene expression of VEGFA and VEGFR-2 was negligible for all surfaces at 24 and 48  
24 h, although it increased considerably after 72 h for all surfaces. An upregulated expression of  
25 VEGFR-2 was statistically significant for NA-CP-RGDS and NA-CP-RGDS+YIGSR series  
26 compared to CT. Concerning VEGFR-1, the gene expression was downregulated in all samples  
27 during time. In fact, at 24 h and 72 h no differences in expression levels were detected between  
28 the different surface treatments. Noteworthy, at 48 h CT-RGDS and NA-CP-RGDS+YIGSR

1 samples showed higher levels of VEGFR -1 gene expression compared to CT and CT-YIGSR,  
2 CT-RGDS+YIGSR, NA-CP-RGDS and NA-CP-YIGSR samples.

#### 4 **Thrombogenicity gene expression**

5 Figures 3 and 4 show the expression of anti-thrombogenic and pro-thrombogenic genes,  
6 respectively, in HUVECs cultured onto physisorbed or functionalized CoCr surfaces. RT-qPCR  
7 measurements revealed that at lower times of cell culture, 24 h, the expression of eNOS  
8 antithrombogenic gene was lower than CT for all tested surfaces; whereas after 48 h the eNOS  
9 gene expression of functionalized surfaces was higher compared to CT but no statistically  
10 significant differences were detected between physisorbed and silanized samples. Finally, at 72  
11 h, the expression level of eNOS was statistically significant higher for silanized surfaces  
12 compared to physisorbed (i.e. CT-RGDS, CT-YIGSR and CT-RGDS+YIGSR) and CT surfaces.  
13 NA-CP-RGDS+YIGSR was the surface with a higher eNOS gene expression at 72 h. tPA gene  
14 expression [Fig. 3(b)] was upregulated after 72 h specially on CT-RGDS, CT-.RGDS+YIGSR  
15 and NA-CP-RGDS+YIGSR compared to control and CT-RGDS, NA-CP-RGDS and NA-CP-  
16 YIGSR.

17 The expression levels of pro-thrombogenic gene PAI-1 [Fig. 4(a)] reached the maximum  
18 expression after 48 h on NA-CP-YIGSR and NA-CP-RGDS+YIGSR but CT and CT-RGDS  
19 and CT-YIGSR showed a considerably decrease. Nevertheless, after 72 h the expression level of  
20 PAI-1 for all surfaces was significantly reduced. The vWF gene expression was downregulated  
21 over time [Fig. 4(b)]. While at 24 h all treated surfaces had lower levels of gene expression  
22 compared to CT, after 48 h the levels were slightly higher for all surfaces. Finally, after 72 h  
23 only NA-CP-RGDS+YIGSR presented higher values compared to CT.

#### 25 **Platelet adhesion**

26 Figure 5(a) shows the percentage of surface covered by platelets and Figure 5(b) the platelets  
27 aggregate size onto TCPS coated with RGDS, YIGSR and RGDS+YIGSR under flow  
28 conditions to determine the potential anti-thrombogenicity of peptides. In general, TCPS coated

1 with peptides lead to a decrease of covered area by platelets and a reduction of the platelet  
2 aggregate size compared to non-coated TCPS. In particular, RGDS coating was the condition  
3 with a lower platelet adhesion compared to YIGSR and RGDS+YIGSR. Moreover, RGDS and  
4 RGDS+YIGSR were the peptide coatings with a lower size of platelet aggregates compared to  
5 YIGSR.

#### 7 **HUVEC and CASMCs co-culture**

8 Figures 6 and 7 display the fluorescence images and the quantification of adhered HUVECs and  
9 SMCs in co-culture after 24h and 48 h onto CT physisorbed and NA silanized CoCr surfaces  
10 with RGDS, YIGSR and their equimolar combination. HUVECs and SMCs showed a capillary-  
11 like morphology after 24 h as seen in Figure 6(a), specially for surfaces functionalized with  
12 YIGSR peptide and the equimolar combination of RGDS and YIGSR. The amount of HUVECs  
13 increased for all the treated surfaces after 48 h compared to 24 h of cell co-culture and  
14 compared to TCPS while SMCs underwent to lower proliferation after 48 h compared to 24 h. It  
15 was also observed an influence of the biomolecules coating since NA-CP-RGDS and NA-CP-  
16 RGDS+YIGSR increased the quantity of adhered HUVEC cells after 24 h (Figure 7). Similarly,  
17 after 48 h CT-YIGSR and NA-CP-RGDS+YIGSR coated surfaces showed higher cell number  
18 compared to the other functionalized surfaces.

#### 20 **DISCUSSION**

21 In this study, surface modified CoCr alloy substrates for cardiovascular applications were  
22 functionalized with RGDS, YIGSR peptides and their equimolar combination by physisorption  
23 and covalent binding via silanization using CPTES as coupling agent. Then, the behavior of  
24 HUVECs cultured onto the different surface finish was evaluated through adhesion,  
25 vascularization, pro-thrombogenic and anti-thrombogenic gene expression.

26 Under normal physiological circumstances, ECs play a major role in preventing blood cells  
27 from adhering to the vasculature and subsequent coagulation.<sup>9</sup> After stent implantation,  
28 interaction of ECs and biomaterial is a crucial step for implant endothelialization. Based on

1 preliminary results, we found that functionalization of peptides (e.g. RGDS, REDV and  
2 YIGSR) onto CoCr surfaces is a promising strategy to overcome this issue.<sup>19</sup> There, we  
3 observed that combination of RGDS and YIGSR stimulated the adhesion of ECs. In addition to  
4 cell adhesion onto biomaterial, the cellular crosstalk through endothelial cell adhesion  
5 molecules such as VCAM-1 and ICAM-1 is also a critical step for endothelial integrity and  
6 functionality.<sup>13,33,34</sup> In the present study, ICAM-1 gene expression increased with time reaching  
7 its highest values for NA-CP-RGDS+YIGSR followed by NA-CP-RGDS and NA-CP-YIGSR  
8 after 72 h. On the other hand, VCAM-1 gene expression was upregulated after 48 h especially  
9 for NA silanized series. These results suggest that RGDS, YIGSR and the equimolar  
10 combination RGDS and YIGSR immobilized by silanization onto CoCr surfaces, could increase  
11 endothelial activation (Table 2). In a previous study, differences in peptide densities between  
12 both silanization and physisorption strategies were described.<sup>19</sup> Moreover, differences could not  
13 be attributed to silanes since no Si 2s was detected after peptides immobilization from X-ray  
14 photoelectron studies.<sup>19</sup> And surface roughness increased from  $\approx 6.3$  nm for CT surfaces to  
15  $\approx 16.0$  nm for CoCr surfaces after NaOH etching. Thus, a higher quantity of immobilized  
16 peptide onto the surface by silanization compared to physisorption could be the reason for the  
17 increase of ICAM-1 and VCAM-1 gene expression.

18 In addition to being indicators of an adequate endothelial integrity, cell adhesion molecules such  
19 as VCAM and ICAM regulate anti-thrombogenic events.<sup>35,36</sup> Their expression in ECs is mainly  
20 regulated by VEGF, a potent angiogenic growth factor secreted by the ECs themselves. The  
21 main activities that VEGF regulates are endothelial cell survival, proliferation, migration, and  
22 tube formation<sup>37</sup> through its recognition via ECs membrane receptors 1 and 2.<sup>37,38</sup> VEGF,  
23 VEGFR-1 and VEGFR-2 are each essential for normal blood vessel development, although  
24 most of the VEGF cellular responses are mediated through the VEGFR-2, including VCAM-1  
25 and ICAM-1 expression regulation.<sup>33</sup> From our results, it was observed a slightly higher  
26 expression of VEGF and VEGFR-2 after 72 h and of VEGFR-1 after 48 h for NA-CP silanized  
27 series compared to CT (Table 2). VEGF stimulation can induce a programmed phenotypic  
28 change of ECs and become pro-thrombotic<sup>38</sup> but this effect is dose dependant. An elevated

1 VEGF concentration can stimulate coagulation and induce EC proliferation and migration in  
2 response to trauma. Nevertheless, a minimum level is needed for the survival of the EC lining.  
3 In our case, NA-CP-RGDS and NA-CP-YIGSR surfaces presented significant higher VEGF  
4 expression compared to CT while NA-CP-RGDS+YIGSR surfaces showed the same VEGF  
5 expression as CT and physisorbed series. Nevertheless the higher expression of ICAM-1 and  
6 VCAM-1 after 72 h and 48 h respectively, onto all silanized NA-CP series independently of the  
7 immobilized peptide compared to CT indicates that the amount of VEGF expressed is low  
8 enough to maintain EC lining.

9 The activation and propagation of the coagulation cascade is mainly prevented by ECs, which  
10 produce and secrete many anti-thrombogenic factors. Among them, endothelial nitric oxide  
11 synthetase (eNOS) which produces nitric oxide that prevents platelet aggregation and  
12 activation;<sup>39</sup> and tissue type plasminogen activator (tPA) converts plasminogen into plasmin for  
13 the immediate breakdown of fibrin.<sup>40,41</sup> In contrast, under pathological conditions they can  
14 secrete pro-thrombogenic factors such as plasminogen activator inhibitor (PAI), which inhibits  
15 the tPA activity, and also the von Willebrand factor which activates the coagulation cascade.<sup>38,42</sup>  
16 The plasminogen activator inhibitor (PAI), a pro-thrombogenic factor, present a higher  
17 upregulation after 48 h onto NA-CP-YIGSR and NA-CP-RGDS+YIGSR surfaces but after 72 h  
18 the expression is reduced. Noteworthy the expression of pro-thrombogenic vWF factor  
19 decreases over time for all surfaces. This behavior is probably related to a healing process  
20 where clot formation is needed for a correct wound healing.

21 Interestingly, the expression of anti-thrombogenic factors tPA and eNOS increased over time.  
22 The NA-CP-RGDS+YIGSR surfaces showed the higher eNOS expression compared to the  
23 other studied surfaces. The fact that the studied pro-thrombogenic genes expression decreases  
24 over time, obtaining insignificant values for PAI-1 and very low values for vWF, combined  
25 with an increase in anti-thrombogenic genes expression over time specially for functionalized  
26 series, indicate that the functionalized surfaces could promote endothelium healing and  
27 functionality and then, prevent thrombogenicity. In particular, the NA-CP-RGDS+YIGSR  
28 treatment seems to be an interesting candidate for accelerating the endothelium recovery.

1  
2  
3 1 Moreover, potential anti-thrombogenicity of peptides was also evaluated through platelet  
4 2 aggregation, by circulating human blood onto TCPS coated surfaces with RGDS, YIGSR and  
5 3 their combination peptides. It is well known that platelet adhesion and aggregation are mediated  
6 4 by fibrinogen via the receptor glycoprotein IIb/IIIa ( $\alpha$ IIb $\beta$ 3), which also recognizes the arginine-  
7 5 glycine-aspartic (RGD) amino-acid sequence.<sup>43</sup> Several authors have demonstrated an inhibitory  
8 6 effect of RGD when is present in solution.<sup>44-46</sup> However, there are few studies concerning the  
9 7 effect of RGD immobilized onto surfaces on platelet adhesion and aggregation. In the present  
10 8 study, surprisingly, platelet adhesion was lower for RGDS peptide compared to TCPS. This  
11 9 reduction in platelet adhesion may be attributed to lower bond interaction between RGDS and  
12 10  $\alpha$ IIb $\beta$ 3 compared to fibrinogen and  $\alpha$ IIb $\beta$ 3,<sup>47</sup> which might be less stable at the applied shear  
13 11 stress in the present study.<sup>48</sup> The different peptides where physisorbed to the TCPS surface,  
14 12 then, a low strength immobilization is expected compared to covalent bonding. This could  
15 13 indicate a detachment of the RGDS to the solution blocking the interaction of  $\alpha$ IIb $\beta$ 3 with  
16 14 fibrinogen thereby reducing the adhesion of platelets. The YIGSR and YIGSR+RGDS peptides  
17 15 also demonstrated lower platelet adhesion values compared to TCPS. In these cases, YIGSR  
18 16 non-specificity for several integrin receptors of platelet cells could be the reason for inhibiting  
19 17 platelet adhesion. Again, a low adhesion of the peptides to the surface could induce a  
20 18 detachment and then, in solution, an interaction with  $\alpha$ IIb $\beta$ 3, decreasing the number of adhered  
21 19 platelets. Noteworthy, all the surfaces covered with peptides demonstrated a lower platelet  
22 20 aggregate size compared to TCPS. This may be attributed to the aforementioned  $\alpha$ IIb $\beta$ 3  
23 21 blocking capacity of the peptides used.

22 22 In addition to ECs activation, communication within SMCs is an essential process for the  
23 23 maintenance of normal tissue physiology.<sup>13,49</sup> The interaction between ECs and SMCs in the  
24 24 artery undoubtedly plays a significant role in vascular wall remodeling and and when it is  
25 25 inadequate could lead to the development of atherosclerotic disease and intimal hyperplasia.  
26 26 However, SMC proliferation at the implant surface is not desired in order to prevent restenosis.  
27 27 In the present work, competition between both types of cells for the modified surfaces was  
28 28 evaluated. At initial co-culture adhesion times, 24 h, the surfaces functionalized with NA-CP-



1  
2  
3 1 RGDS and NA-CP-RGDS+YIGSR showed a higher number of adhered HUVECs compared to  
4  
5 2 the other tested surfaces. However after 48 h of cell co-culture CT-YIGSR and NA-CP-  
6  
7 3 RGDS+YIGSR series showed the higher HUVEC adhesion. This indicates that the equimolar  
8  
9 4 combination of RGDS and YIGSR immobilized onto CoCr surface, exhibit adhesion selectivity  
10  
11 5 toward ECs. Therefore, an interesting synergistic effect is observed between both RGDS and  
12  
13 6 YIGSR active sequences. This synergistic effect may be attributed to the fact that both RGDS  
14  
15 7 and YIGSR peptides interact with different cell receptor molecules. Whereas the former is an  
16  
17 8 integrin binding sequence the later interacts with the 67 kDa laminin binding protein (LBP). It  
18  
19 9 is well known that RGDS modified surfaces allow the formation of focal adhesion sites  
20  
21 10 promoting cell spreading.<sup>50,51</sup> Interestingly, the YIGSR peptide has been found to co-localize  
22  
23 11 LBP with  $\alpha$ -actinin and vinculin acting as an integrin-accessory molecule that contributes to the  
24  
25 12 formation of focal adhesion.<sup>52</sup> In addition, activation of LBP by laminin or laminin peptides (i.e.  
26  
27 13 YIGSR) has been related not only to cell attachment but also to cell differentiation, migration  
28  
29 14 and capillary-like structures formation.<sup>53</sup> Generally, functionalization increased the amount of  
30  
31 15 adhered HUVEC cells onto modified CoCr surfaces compared to plain CoCr, CT, independently  
32  
33 16 of the peptide used and the strategy of immobilization. Moreover, a considerably lower amount  
34  
35 17 of adhered CASMCs compared to adhered HUVECs in all surfaces was found. These results are  
36  
37 18 in agreement with our preliminary results of ECs and SMCs single cell culture where an  
38  
39 19 enhancement of HUVEC adhesion and proliferation on the adhered biomolecules onto CoCr  
40  
41 20 was found while controlling SMC adhesion.<sup>19</sup> Herein, a higher number of ECs after 4h of  
42  
43 21 culture compared to SMCs was observed. This competition for the functionalized surfaces could  
44  
45 22 be critical for SMCs in co-culture conditions where ECs adhere faster probably sequestering  
46  
47 23 potential SMC adhesion motifs. In addition, another possible explanation for such behavior is  
48  
49 24 that both ECs and SMCs need an optimal peptide concentration for effective adhesion<sup>54</sup> that is  
50  
51 25 probably not achieved for satisfactory supporting SMC adhesion.  
52  
53  
54  
55

## 56 CONCLUSIONS

57  
58 28 We analysed the effect of immobilizing RGDS and YIGSR peptides, and their equimolar  
59  
60



1  
2  
3 1 combination on CoCr surfaces to determine HUVECs adhesion gene expression,  
4  
5 2 thrombogenicity and HUVEC/CASMC co-culture. The results suggested the positive effect of  
6  
7 3 functionalized surfaces to enhance HUVECs adhesion also in co-culture with SMCs, and the  
8  
9 4 decrease of thrombogenicity depending on the surface finish. Taking all together, the equimolar  
10  
11 5 combination of RGDS and YIGSR seems to be the most promising strategy for  
12  
13 6 endothelialization of CoCr surfaces as observed by the gene expression of genes related to  
14  
15 7 adhesion, vascularization, anti-thrombogenic processes in HUVECs. Cell adhesive peptides  
16  
17 8 functionalization of CoCr metallic surfaces for cardiovascular applications may offer an  
18  
19 9 efficient alternative to enhance rapid endothelialization, while preventing restenosis and  
20  
21 10 thrombosis.  
22  
23  
24  
25

## 26 **ACKNOWLEDGMENTS**

27  
28 13 Authors acknowledge the Spanish Government for financial support through project MAT2015-  
29  
30 14 67183-R (MINECO/FEDER), and the Agency for Administration of University and Research  
31  
32 15 Grants of the Government of Catalonia (2014 SGR 1333). M.P. acknowledges the Health  
33  
34 16 Institute Carlos III (ISCIII): Health Technological Development project DTS16/00133  
35  
36 17 (MINECO/FEDER). M.I.C. would like to thank the Government of Catalonia for funding  
37  
38 18 through a FI Scholarship. Support for the research of M.P.G. was received through the prize  
39  
40 19 “ICREA Academia” for excellence in research, funded by the Generalitat de Catalunya.  
41  
42  
43  
44  
45  
46  
47  
48  
49  
50  
51  
52  
53  
54  
55  
56  
57  
58  
59  
60

1  
2  
3 **REFERENCES**

- 4 1. Packard RRS, Libby P. Inflammation in Atherosclerosis: From Vascular Biology to  
5 Biomarker Discovery and Risk Prediction. *Clin Chem.* 2007;54:24–38.  
6  
7 2. Meadows A, Bhatt DL. Clinical aspects of platelet inhibitors and thrombus formation.  
8 *Circ Res.* 2007; 100: 1261-1275.  
9  
10 3. Andukuri A, Minor WP, Kushwaha M, Anderson JM, Jun HW. Effect of endothelium  
11 mimicking self-assembled nanomatrices on cell adhesion and spreading of human  
12 endothelial cells and smooth muscle cells. *Nanomedicine Nanotechnology, Biol Med.*  
13 2010;6:289–97.  
14  
15 4. Puranik AS, Dawson ER, Peppas N a. Recent advances in drug eluting stents. *Int J*  
16 *Pharm.* 2013; 441: 665-679.  
17  
18 5. Nakazawa G, Finn A V., Vorpahl M, Ladich ER, Kolodgie FD, Virmani R. Coronary  
19 responses and differential mechanisms of late stent thrombosis attributed to first-  
20 generation sirolimus- and paclitaxel-eluting stents. *J Am Coll Cardiol.* 2011;57:390–98.  
21  
22 6. Ellis SG, Savage M, Fischman D, Baim DS, Leon M, Goldberg S, Hirshfeld JW, Cleman  
23 MW, Teirstein PS, Walker C. Restenosis after placement of Palmaz-Schatz stents in  
24 native coronary arteries. Initial results of a multicenter experience. *Circulation.*  
25 1992;86:1836–44.  
26  
27 7. Padfield GJ, Newby DE, Mills NL. Understanding the role of endothelial progenitor  
28 cells in percutaneous coronary intervention. *J Am Coll Cardiol.* 2010;55:1553–65.  
29  
30 8. Costa MA, Simon DI. Molecular basis of restenosis and drug-eluting stents. *Circulation.*  
31 2005;111:2257–73.  
32  
33 9. Otsuka F, Finn A V., Yazdani SK, Nakano M, Kolodgie FD, Virmani R. The importance  
34 of the endothelium in atherothrombosis and coronary stenting. *Nat Rev Cardiol.*  
35 2012;9:439–53.  
36  
37 10. Kouvroukoglou S, Dee KC, Bizios R, McIntire L V., Zygourakis K. Endothelial cell  
38 migration on surfaces modified with immobilized adhesive peptides. *Biomaterials.*  
39 2000;21:1725–33.  
40  
41  
42  
43  
44  
45  
46  
47  
48  
49  
50  
51  
52  
53  
54  
55  
56  
57  
58  
59  
60

- 1  
2  
3 1 11. de Mel A, Jell G, Stevens MM, Seifalian AM. Biofunctionalization of biomaterials for  
4 accelerated in situ endothelialization: A review. *Biomacromolecules*. 2008.  
5 2  
6 3 12. Nazneen F, Herzog G, Arrigan DWM, Caplice N, Benvenuto P, Galvin P, Thompson M.  
7 Surface chemical and physical modification in stent technology for the treatment of  
8 coronary artery disease. *J Biomed Mater Res B Appl Biomater*. 2012;100:1989–2014.  
9 4  
10 5 13. Heng BC, Bezerra PP, Meng QR, Chin DW-L, Koh LB, Li H, Zhang H, Preiser PR,  
11 Boey FY-C, Venkatraman SS. Adhesion, proliferation, and gene expression profile of  
12 human umbilical vein endothelial cells cultured on bilayered polyelectrolyte coatings  
13 composed of glycosaminoglycans. *Biointerphases*. 2010;5:53–62.  
14 6  
15 10 14. Kumar TRS, Krishnan LK. Fibrin-mediated endothelial cell adhesion to vascular  
16 biomaterials resists shear stress due to flow. *J Mater Sci Mater Med*. 2002;13:751–5.  
17 11  
18 12 15. Sargeant TD, Rao MS, Koh CY, Stupp SI. Covalent functionalization of NiTi surfaces  
19 with bioactive peptide amphiphile nanofibers. *Biomaterials*. 2008;29:1085–98.  
20 13  
21 14 16. Khazaei M, Moien-afshari F, Laher I. Vascular endothelial function in health and  
22 diseases. *Pathophysiology*. 2008;15:49–67.  
23 15  
24 16 17. Frank PG, Pavlides S, Lisanti MP. Caveolae and transcytosis in endothelial cells: role in  
25 atherosclerosis. *Cell Tissue Res*. 2009;335:41–7.  
26 17  
27 18 18. Simionescu M, Antohe F. Functional ultrastructure of the vascular endothelium:  
28 Changes in various pathologies. *Handb Exp Pharmacol*. 2006;176:41–69.  
29 19  
30 20 19. Castellanos MI, Mas-Moruno C, Grau A, Serra-Picamal X, Trepal X, Albericio F, Joner  
31 M, Gil FJ, Ginebra MP, Manero JM, Pegueroles M. Functionalization of CoCr surfaces  
32 with cell adhesive peptides to promote HUVECs adhesion and proliferation. *Appl Surf  
33 Sci*. 2017;393:82–92.  
34 21  
35 24 20. Sarfati G, Dvir T, Elkabets M, Apte RN, Cohen S. Targeting of polymeric nanoparticles  
36 to lung metastases by surface-attachment of YIGSR peptide from laminin. *Biomaterials*.  
37 2011;32:152–61.  
38 25  
39 27 21. Sriramarao P, Mendler M, Bourdon MA. Endothelial cell attachment and spreading on  
40 human tenascin is mediated by alpha 2 beta 1 and alpha v beta 3 integrins. *J Cell Sci*  
41 28

- 1  
2  
3 1 1993;1012:1001–12.  
4  
5 22. Graf J, Ogle RC, Robey F a, Sasaki M, Martin GR, Yamada Y, Kleinman HK. A  
6  
7 3 pentapeptide from the laminin B1 chain mediates cell adhesion and binds the 67,000  
8  
9 4 laminin receptor. *Biochemistry*. 1987;26:6896–900.  
10  
11 23. Shenkman B, Einav Y, Salomon O, Varon D, Savion N. Testing agonist-induced platelet  
12  
13 6 aggregation by the Impact-R [Cone and plate(let) analyzer (CPA)]. *Platelets*.  
14  
15 7 2008;19:440–6.  
16  
17 24. Mas-Moruno C, Fraioli R, Albericio F, Manero JM, Gil FJ. A Novel peptide-based  
18  
19 9 platform for the dual presentation of biologically-active peptide motifs on biomaterials.  
20  
21 10 *ACS Appl Mater Interfaces*. 2014;6:6525–36.  
22  
23 25. Habibzadeh S, Li L, Omanovic S, Shum-Tim D, Davis EC. Biocompatibility of Ir/Ti-  
24  
25 12 oxide coatings: Interaction with platelets, endothelial and smooth muscle cells. *Appl*  
26  
27 13 *Surf Sci*. 2014;301:530–8.  
28  
29 14 26. Ding Y, Yang Z, Bi CWC, Yang M, Zhang J, Xu SL, Lu X, Huang N, Huang P, Leng Y.  
30  
31 15 Modulation of protein adsorption, vascular cell selectivity and platelet adhesion by  
32  
33 16 mussel-inspired surface functionalization. *J Mater Chem B*. 2014 [;2:3819–29.  
34  
35 17 27. Castellanos MI, Gil FJ, Manero JM, Pegueroles M. Biofunctionalization of REDV  
36  
37 18 elastin-like recombinamers on a CoCr surface selective improves endothelialization for  
38  
39 19 cardiovascular applications. *Colloids Surfaces B Biointerfaces*. 2015;127:22–32.  
40  
41 20 28. Rocas P, Hoyos-Nogués M, Rocas J, Manero JM, Gil J, Albericio F, Mas-Moruno C.  
42  
43 21 Installing Multifunctionality on Titanium with RGD-Decorated Polyurethane-Polyurea  
44  
45 22 Roxithromycin Loaded Nanoparticles: Toward New Osseointegrative Therapies. *Adv*.  
46  
47 23 2015;4:1956–60.  
48  
49 24 29. Fraioli R, Rechenmacher F, Neubauer S, Manero JM, Gil J, Kessler H, Mas-Moruno C.  
50  
51 25 Mimicking bone extracellular matrix: Integrin-binding peptidomimetics enhance  
52  
53 26 osteoblast-like cells adhesion, proliferation, and differentiation on titanium. *Colloids*  
54  
55 27 *Surfaces B Biointerfaces*. 2015;128:191–200.  
56  
57 28 30. Guillem-Marti J, Delgado L, Godoy-Gallardo M, Pegueroles M, Herrero M, Gil FJ.

- 1  
2  
3 1 Fibroblast adhesion and activation onto micro-machined titanium surfaces. *Clin Oral*  
4  
5 2 *Implants Res.* 2013;24:770–80.  
6  
7 31. Varon D, Dardik R, Shenkman B, Kotev-Emeth S, Farzame N, Tamarin I, Savion N. A  
8  
9 4 new method for quantitative analysis of whole blood platelet interaction with  
10  
11 5 extracellular matrix under flow conditions. *Thromb Res.* 1997;85:283–94.  
12  
13 6 32. Hsieh C-Y, Chen C-L, Yang K-C, Ma C-T, Choi P-C, Lin C-F. Detection of Reactive  
14  
15 7 Oxygen Species During the Cell Cycle Under Normal Culture Conditions Using a  
16  
17 8 Modified Fixed-Sample Staining Method. *J Immunoassay Immunochem.* 2014;1819:37–  
18  
19 9 41.  
20  
21 10 33. Kim I, Moon SO, Kim SH, Kim HJ, Koh YS, Koh GY. Vascular endothelial growth  
22  
23 11 factor expression of intercellular adhesion molecule 1 (ICAM-1), vascular cell adhesion  
24  
25 12 molecule 1 (VCAM-1), and E-selectin through nuclear factor-kappa B activation in  
26  
27 13 endothelial cells. *J Biol Chem.* 2001;276:7614–20.  
28  
29 14 34. Videm V, Albrigtsen M. Soluble ICAM-1 and VCAM-1 as markers of endothelial  
30  
31 15 activation. *Scand J Immunol.* 2008;67:523–31.  
32  
33 16 35. McGuigan AP, Sefton M V. The influence of biomaterials on endothelial cell  
34  
35 17 thrombogenicity. *Biomaterials.* 2007;28:2547–71.  
36  
37 18 36. Pepinsky B, Hession C, Chen LL, Moy P, Burkly L, Jakubowski A, Chow EP, Benjamin  
38  
39 19 C, Chi-Rosso G, Luhowskyj S. Structure/function studies on vascular cell adhesion  
40  
41 20 molecule-1. *J Biol Chem.* 1992;267:17820–6.  
42  
43 21 37. Ferrara N, Davis-smyth T. The Biology of Vascular Endothelial Growth Factor.  
44  
45 22 2013;18:4–25.  
46  
47 23 38. Verheul HMW, Pinedo HM. Possible molecular mechanisms involved in the toxicity of  
48  
49 24 angiogenesis inhibition. *Nat Rev Cancer.* 2007;7:475–85.  
50  
51 25 39. Sessa WC. eNOS at a glance. *J Cell Sci.* 2004;117:2427–9.  
52  
53 26 40. Stricker RB, Wong D, Shiu DT, Reyes PT, Shuman MA. Activation of plasminogen by  
54  
55 27 tissue plasminogen activator on normal and thrombasthenic platelets: effects on surface  
56  
57 28 proteins and platelet aggregation. *Blood.* 1986;68:275–80.  
58  
59  
60

- 1  
2  
3 1 41. Hoylaerts M, Rijken DC, Lijnen HR, Collen D. Kinetics of the activation of  
4 plasminogen by human tissue plasminogen activator. Role of fibrin. *J Biol Chem*.  
5 1982;257:2912–9.  
6  
7  
8  
9 42. Bombeli T, Schwartz BR, Harlan JM. Adhesion of activated platelets to endothelial  
10 cells: evidence for a GPIIbIIIa-dependent bridging mechanism and novel roles for  
11 endothelial intercellular adhesion molecule 1 (ICAM-1), alphavbeta3 integrin, and  
12 GPIIbIIIa. *J Exp Med*. 1998;187:329–39.  
13  
14  
15  
16  
17 43. Rubin BG, McGraw DJ, Sicard GA, Santoro SA, D P, Louis S. New RGD analogue  
18 inhibits human platelet adhesion and aggregation and eliminates platelet deposition on  
19 canine vascular grafts. *J Vasc Surg*. 1992;15:683–92.  
20  
21  
22  
23 44. Chen CS, Papayannopoulos IA, Timmons S, Chou SH, Thiagarajan P. A modified Arg-  
24 Asp-Val (RDV) peptide derived during the synthesis of Arg-Glu-Asp-Val (REDV), a  
25 tetrapeptide derived from an alternatively spliced site in fibronectin, inhibits the binding  
26 of fibrinogen, fibronectin, von Willebrand factor and vitronectin t. *BBA - Gen Subj*.  
27 ASBMB; 1991;1075:237–47.  
28  
29  
30  
31  
32  
33 45. Plow EF, D'Souza SE, Ginsberg MH. Ligand binding to GPIIb-IIIa: a status report.  
34 *Semin Thromb Hemost*. 1992;18(3):324-32.  
35  
36  
37  
38 46. Pollina E. Design and synthesis of RGD mimetics as potent inhibitors of platelet  
39 aggregation. *J Undergrad Sci*. 1996;3:119–26.  
40  
41  
42 47. Müller B, Zerwes HG, Tangemann K, Peter J, Engel J. Two-step binding mechanism of  
43 fibrinogen to alpha IIb beta 3 integrin reconstituted into planar lipid bilayers. *J Biol*  
44 *Chem*. 1993;268:6800–8.  
45  
46  
47  
48 48. Goldsmith HL, McIntosh FA, Shahin J, Frojmovic MM. Time and force dependence of  
49 the rupture of glycoprotein IIb-IIIa-fibrinogen bonds between latex spheres. *Biophys J*.  
50 2000;78:1195–206.  
51  
52  
53  
54 49. Ouaiissi A, Capron A. Some aspects of protozoan parasite-host cell interactions with  
55 special reference to RGD-mediated recognition process. *Microb Pathog*. 1989.  
56  
57  
58 50. Hersel U. RGD modified polymers: biomaterials for stimulated cell adhesion and  
59  
60

- 1  
2  
3 1 beyond. *Biomaterials*. 2003;24:4385–415.  
4  
5 2 51. Pierschbacher MD, Ruoslahti E. Cell attachment activity of fibronectin can be duplicated  
6  
7 3 by small synthetic fragments of the molecule. *Nature*. 1984;30–3.  
8  
9 4 52. Massia SP, Rao SS, Hubbell JA. Covalently immobilized laminin peptide Tyr-Ile-Gly-  
10  
11 5 Ser-Arg (YIGSR) supports cell spreading and co-localization of the 67-kilodalton  
12  
13 6 laminin receptor with  $\alpha$ -actinin and vinculin. *J Biol Chem*. 1993;268:8053–9.  
14  
15 7 53. Ménard S, Castronovo V, Tagliabue E, Sobel ME. New insights into the metastasis-  
16  
17 8 associated 67 kD laminin receptor. *J Cell Biochem*. 1997;67:155–65.  
18  
19 9 54. Fittkau MH, Zilla P, Bezuidenhout D, Lutolf MP, Human P, Hubbell JA, Davies N. The  
20  
21 10 selective modulation of endothelial cell mobility on RGD peptide containing surfaces by  
22  
23 11 YIGSR peptides. *Biomaterials*. 2005;26:167–74.  
24  
25 12  
26  
27  
28  
29  
30  
31  
32  
33  
34  
35  
36  
37  
38  
39  
40  
41  
42  
43  
44  
45  
46  
47  
48  
49  
50  
51  
52  
53  
54  
55  
56  
57  
58  
59  
60

1  
2  
3 **1 FIGURES LEGENDS**

4  
5 **2 FIGURE 1.** Real time – qPCR analyses of the gene expressions for the selected genes of  
6  
7 adhesion: a) ICAM-1 and b) VCAM-1 in HUVEC cultured on CT physisorbed and NA  
8  
9 chemisorbed modified CoCr surfaces for 24, 48 and 72h. Results were normalized in respect to  
10  
11 expression levels of the endogen reference gene  $\beta$ -actin and are represented as relative fold  
12  
13 change to CT at 24 h (as explained in Materials and Methods section). For each studied gene,  
14  
15 the letters a, b, c, d, e, f join surfaces with non-significant differences ( $p < 0.05$ ).  
16  
17

18  
19 **8 FIGURE 2.** Real time – qPCR analyses of the gene expressions for the selected genes of  
20  
21 vascularization: a) VEGFA, b) VEGFR-1 and c) VEGFR-2 in HUVEC cultured on CT  
22  
23 physisorbed and NA chemisorbed modified CoCr surfaces for 24, 48 and 72h. Results were  
24  
25 normalized in respect to expression levels of the endogen reference gene  $\beta$ -actin and are  
26  
27 represented as relative fold change to CT at 24 h (as explained in Materials and Methods  
28  
29 section). For each studied gene, the letters a, b, c, d, e, f join surfaces with non-significant  
30  
31 differences ( $p < 0.05$ ).  
32  
33

34  
35 **15 FIGURE 3.** Real time – qPCR analyses of the gene expressions for the selected genes of anti-  
36  
37 thrombogenic: a) eNOS and b) tPA in HUVEC cultured on CT physisorbed and NA  
38  
39 chemisorbed modified CoCr surfaces for 24, 48 and 72h. Results were normalized in respect to  
40  
41 expression levels of the endogen reference gene  $\beta$ -actin and are represented as relative fold  
42  
43 change to CT at 24 h (as explained in Materials and Methods section). For each studied gene,  
44  
45 the letters a, b, c, d join surfaces with non-significant differences ( $p < 0.05$ ).  
46

47  
48 **21 FIGURE 4.** Real time – qPCR analyses of the gene expressions for the selected genes of pro-  
49  
50 thrombogenic: a) PAI-1 and b) vWF in HUVEC cultured on CT physisorbed and NA  
51  
52 chemisorbed modified CoCr surfaces for 24, 48 and 72h. Results were normalized in respect to  
53  
54 expression levels of the endogen reference gene  $\beta$ -actin and are represented as relative fold  
55  
56 change to CT at 24 h (as explained in Materials and Methods section). For each studied gene,  
57  
58 the letters a, b, c, d join surfaces with non-significant differences ( $p < 0.05$ ).  
59  
60



1  
2  
3 1 **FIGURE 5.** Platelet adhesion assay, on TCPS coated with RGDS, YIGSR and the equimolar  
4  
5 2 combination RGDS+YIGSR evaluated by exposing human blood to physiological arterial shear  
6  
7 3 stress. The symbols join surfaces with non-statistically significant differences ( $p < 0.05$ ).  
8

9  
10 4 **FIGURE 6.** Overall morphology of adhered HUVEC (green) and SMC (red) cells co-cultured  
11  
12 5 on a) CT physisorbed b) NA-CP silanized biofunctionalized surfaces after 24 and 48 h and  
13  
14 6 visualized by fluorescence microscopy. Bars: 50  $\mu\text{m}$ .  
15

16  
17 7 **FIGURE 7.** Quantification adhered HUVEC and SMC cells co-cultured on CT physisorbed and  
18  
19 8 NA-CP silanized biofunctionalized surfaces after 24 and 48 h.  
20

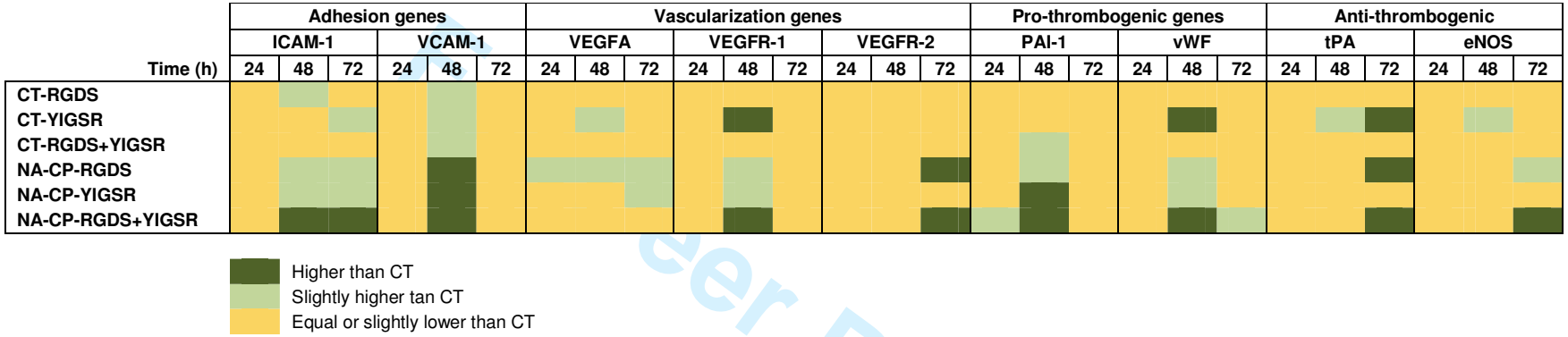
21  
22 9  
23  
24  
25  
26  
27  
28  
29  
30  
31  
32  
33  
34  
35  
36  
37  
38  
39  
40  
41  
42  
43  
44  
45  
46  
47  
48  
49  
50  
51  
52  
53  
54  
55  
56  
57  
58  
59  
60

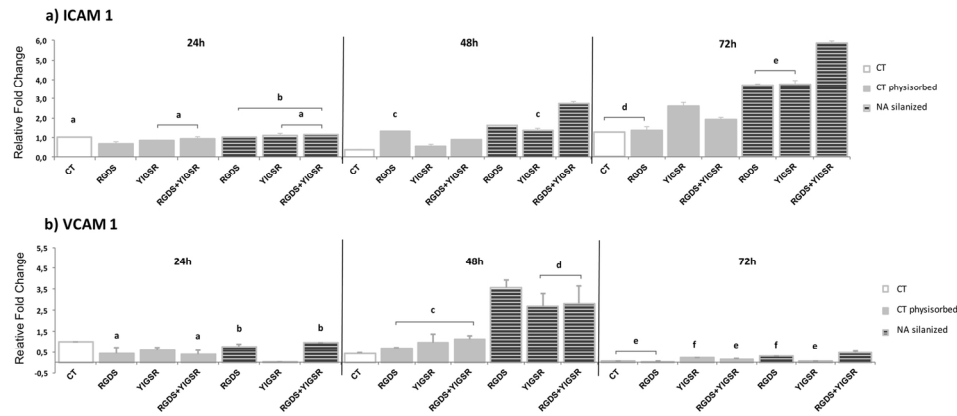
Table 1. DNA sequences of forward (fw) and reverse (rv) primers for the selected genes used for real-time qPCR

Related function	Gene Symbol	Gene title	Acc. Number	Primer sequences	Amplicon size (bp)
Adhesion	ICAM-1	Intercellular adhesion molecule	NM_000201.2	fw:CCTTCCTCACCGTGTACTGG rv:AGCGTAGGGTAAGGTTCTTGC	90
	VCAM-1	Vascular adhesion molecule	NM_0001078.3	fw: CATGGAATTCGAACCCAAAC rv: TGTATCTCTGGGGCAACA	70
Vascularization	VEGFA	Vascular endothelial growth factor A	NM_001025370.2	fw: CCTCCGAAACCATGAACTTT rv: ATGATTCTGCCCTCCTCCTT	122
	VEGFR-1	Vascular endothelial growth factor receptor-1	NM_002019.4	fw:CAGCATACTCACTGTTCAAGG rv: CCACACAGGTGCATGTTAGAG	75
	VEGFR-2	Vascular endothelial growth factor receptor-2	NM_002253.2	fw: CGCATCACATCCACTGGTATT rv: TTTGTCACTGAGACAGCTTGG	76
Pro-thrombotic	PAI-1	Plasminogen activator inhibitor	NM_00062.3	fw:AAGGCACCTCTGAGAATTCA rv: CCCAGGACTAGGCAGGTG	61
	vWF	von Willebrand Factor	NM_000552.3	fw: GAAATGTGTCAGGAGCGATG rv:ATCCAGGAGCTGTCCCTCA	60
Anti-thrombotic	eNOS	Endothelial Nitric oxide-synthetase	NM_001160109.1	fw: GCATCCCTACTCCCACCAG rv:TTCTTACACGAGGGAACTTG	92
	tPA	Plasminogen activator	NM_000930.3	fw:AGCTGTGGGGAGCTCAGA rv:CACAGCGTCCCTTAAATTCAC	105
House keeping	$\beta$ -actin	Beta actin	NM_001101.3	fw: AGAGCTACGAGCTGCCTGAC rv: CGTGGATGCCACAGGACT	114

1  
2  
3  
4  
5  
6  
7  
8  
9  
10  
11  
12  
13  
14  
15  
16  
17  
18  
19  
20  
21  
22  
23  
24  
25  
26  
27  
28  
29  
30  
31  
32  
33  
34  
35  
36  
37  
38  
39  
40  
41  
42  
43  
44  
45  
46  
47  
48  
49

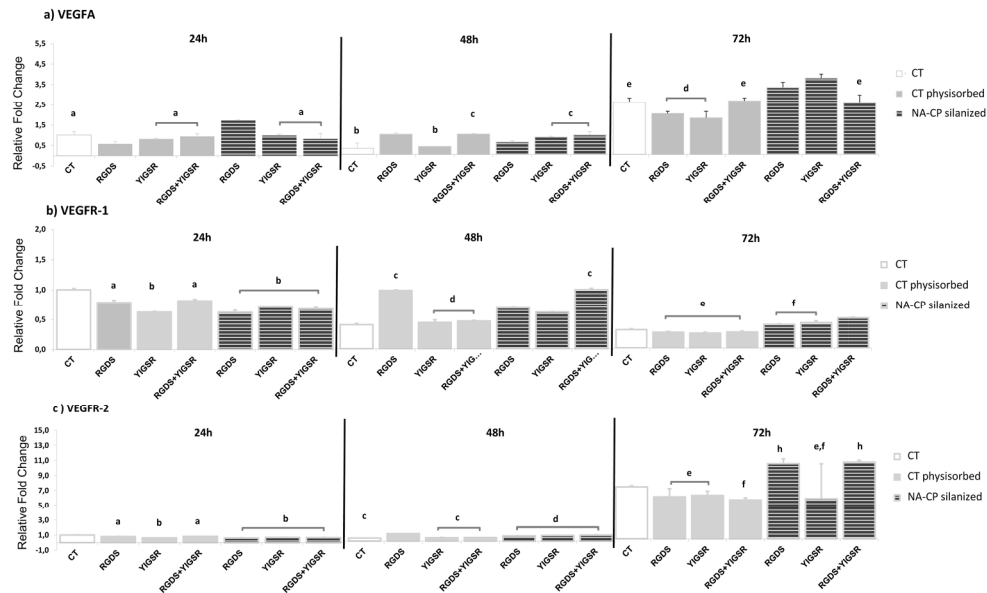
Table 2. Summary of the gene expression analysis of CT physisorbed and NA-CP chemisorbed modified CoCr surfaces





Real time – qPCR analyses of the gene expressions for the selected genes of adhesion: a) ICAM-1 and b) VCAM-1 in HUVEC cultured on CT physisorbed and NA chemisorbed modified CoCr surfaces for 24, 48 and 72h. Results were normalized in respect to expression levels of the endogen reference gene  $\beta$ -actin and are represented as relative fold change to CT at 24 h (as explained in Materials and Methods section). For each studied gene, the letters a, b, c, d, e, f join surfaces with non-significant differences ( $p < 0.05$ ).

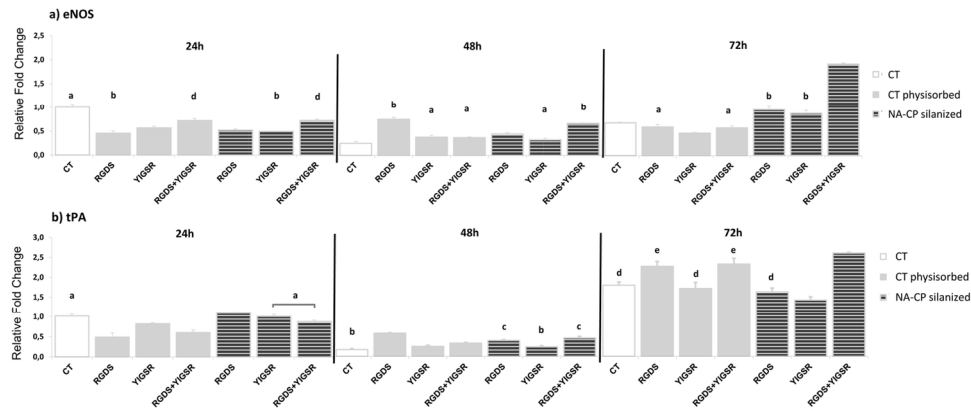
Figure 1  
147x64mm (300 x 300 DPI)



Real time - qPCR analyses of the gene expressions for the selected genes of vascularization: a) VEGFA, b) VEGFR-1 and c) VEGFR-2 in HUVEC cultured on CT physisorbed and NA chemisorbed modified CoCr surfaces for 24, 48 and 72h. Results were normalized in respect to expression levels of the endogen reference gene  $\beta$ -actin and are represented as relative fold change to CT at 24 h (as explained in Materials and Methods section). For each studied gene, the letters a, b, c, d, e, f join surfaces with non-significant differences ( $p < 0.05$ ).

Figure 2

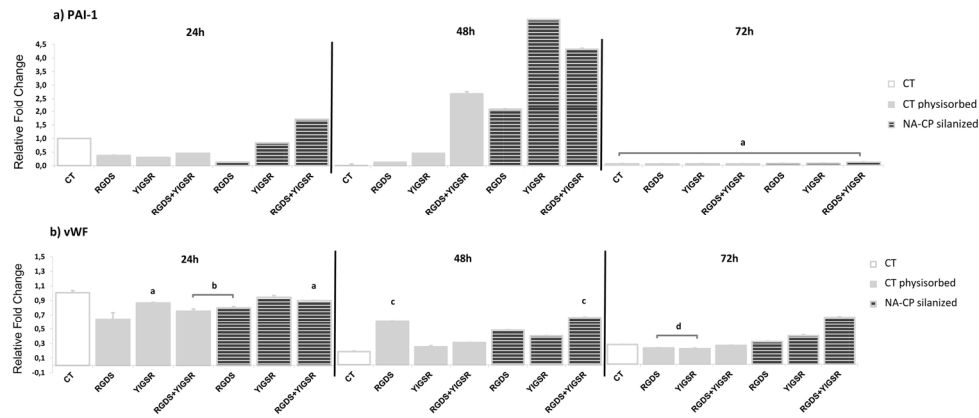
205x124mm (300 x 300 DPI)



Real time - qPCR analyses of the gene expressions for the selected genes of anti-thrombogenic: a) eNOS and b) tPA in HUVEC cultured on CT physisorbed and NA chemisorbed modified CoCr surfaces for 24, 48 and 72h. Results were normalized in respect to expression levels of the endogen reference gene  $\beta$ -actin and are represented as relative fold change to CT at 24 h (as explained in Materials and Methods section). For each studied gene, the letters a, b, c, d join surfaces with non-significant differences ( $p < 0.05$ ).

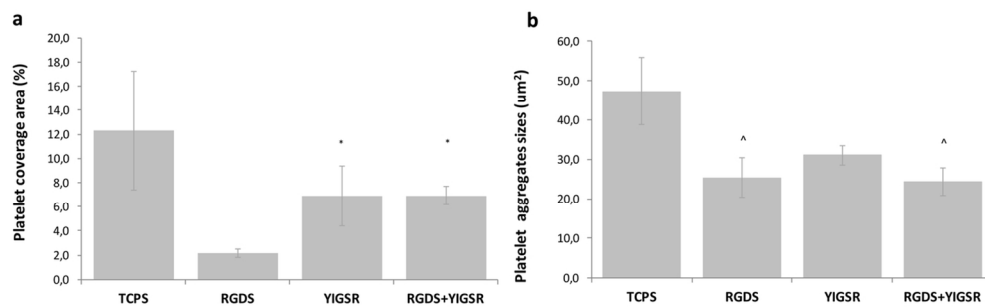
Figure 3

140x58mm (300 x 300 DPI)



Real time - qPCR analyses of the gene expressions for the selected genes of pro-thrombogenic: a) PAI-1 and b) vWF in HUVEC cultured on CT physisorbed and NA chemisorbed modified CoCr surfaces for 24, 48 and 72h. Results were normalized in respect to expression levels of the endogen reference gene  $\beta$ -actin and are represented as relative fold change to CT at 24 h (as explained in Materials and Methods section). For each studied gene, the letters a, b, c, d join surfaces with non-significant differences ( $p < 0.05$ ).

Figure 4  
175x75mm (300 x 300 DPI)



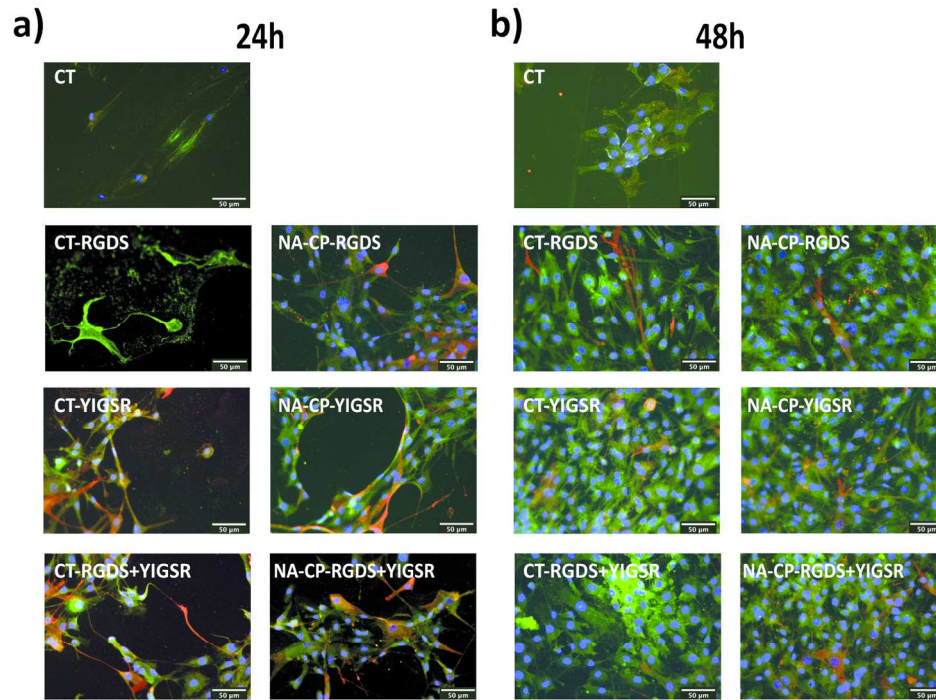
Platelet adhesion assay, on TCPS coated with RGDS, YIGSR and the equimolar combination RGDS+YIGSR evaluated by exposing human blood to physiological arterial shear stress. The symbols join surfaces with non-statistically significant differences ( $p < 0.05$ ).

Figure 5

118x36mm (300 x 300 DPI)

Peer Review



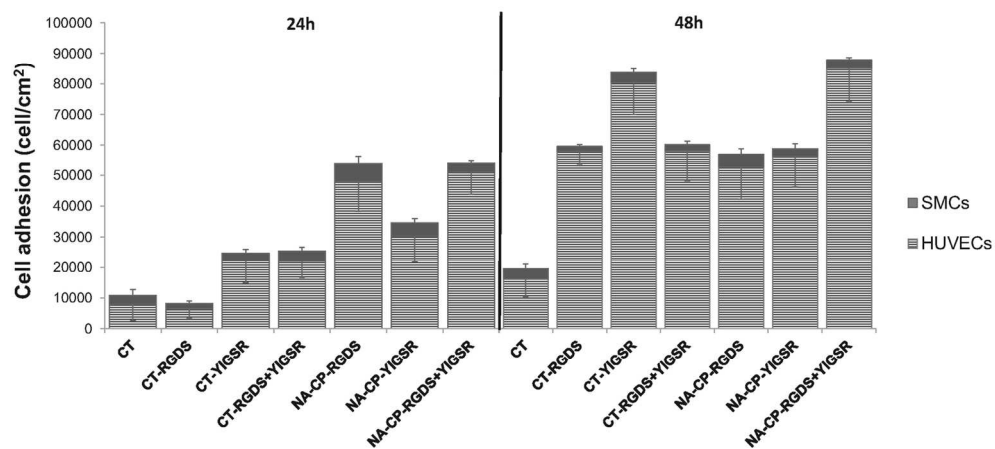


32 Overall morphology of adhered HUVEC (green) and SMC (red) cells co-cultured on a) CT physisorbed b) NA-CP silanized biofunctionalized surfaces after 24 and 48 h and visualized by fluorescence microscopy. Bars: 50 μm.

34 Figure 6

35 165x122mm (300 x 300 DPI)

36  
37  
38  
39  
40  
41  
42  
43  
44  
45  
46  
47  
48  
49  
50  
51  
52  
53  
54  
55  
56  
57  
58  
59  
60  
view



Quantification adhered HUVEC and SMC cells co-cultured on CT physisorbed and NA-CP silanized biofunctionalized surfaces after 24 and 48 h.

Figure 7

147x72mm (300 x 300 DPI)